

A simple protocol for the probability weights of the simulated tempering algorithm: applications to first-order phase transitions

Carlos E. Fiore^{1, a)} and M. G. E. da Luz^{1, b)}

*Departamento de Física, Universidade Federal do Paraná, CP 19044,
81531-990 Curitiba, Brazil*

(Dated: 11 November 2010)

The simulated tempering (ST) is an important method to deal with systems whose phase spaces are hard to sample ergodically. However, it uses accepting probabilities weights which often demand involving and time consuming calculations. Here it is shown that such weights are quite accurately obtained from the largest eigenvalue of the transfer matrix – a quantity straightforward to compute from direct Monte Carlo simulations – thus simplifying the algorithm implementation. As tests, different systems are considered, namely, Ising, Blume-Capel, Blume-Emery-Griffiths and Bell-Lavis liquid water models. In particular, we address first-order phase transition at low temperatures, a regime notoriously difficult to simulate because the large free-energy barriers. The good results found (when compared with other well established approaches) suggest that the ST can be a valuable tool to address strong first-order phase transitions, a possibility still not well explored in the literature.

PACS numbers: 05.10.Ln, 05.70.Fh, 05.50.+q

Keywords: simulated tempering, first-order phase transitions, eigenvalues of the transfer matrix, Ising and lattice-gas models

^{a)}Electronic mail: fiore@fisica.ufpr.br

^{b)}Electronic mail: luz@fisica.ufpr.br

I. INTRODUCTION

Many statistical systems are difficult to “probe” since their phase spaces display complicated landscapes full of energetic valleys and hills^{1,2}. In such case, a non-representative sampling of the microstates, e.g., due to uneven visits to the different domains³, can lead to metastability and broken ergodicity, with a consequent non-convergence to equilibrium and poor estimates for the thermodynamic quantities^{4,5}. This is exactly the situation found in first-order phase transitions⁶, where the free-energy minima are separated by large barriers, and simple one-flip Metropolis approaches are unable to solve the problem.

Thus, different methods – aimed to guarantee ergodic simulations in the context described above – have been proposed^{7–13}. Among the so called enhanced sampling algorithms, a particularly important one due to its simplicity and generality is the simulated tempering (ST)^{14,15} (closely related to the also relevant parallel (or replica) tempering, PT, approach¹⁶). Here, tempering means that along the simulations the system can undergo temperature changes. Consider we shall analyze a system at $T = T_1$. Besides an usual Monte Carlo (MC) prescription, in the ST algorithm T is also treated as a dynamical variable: the temperature can assume distinct values from a set $\{T_1 < T_2 < \dots < T_N\}$, switching from time to time according to established accepting probabilities p 's. Of course, during the simulations the relevant averages necessary to obtain the sought thermodynamic quantities are performed only when the system is at T_1 . The central idea is that temporary evolutions at higher T 's strongly facilitates the crossing of the free-energy barriers, then allowing uniform visits to the multiple regions of a fragmented phase-space¹⁷.

A fundamental ingredient in the ST is the definition of the accepting probabilities¹⁴; functions of the energy, the different T 's and appropriate weight factors g (see next Section as well as interesting discussions in Ref.¹⁸). By their turn, the exact expressions for the g 's depend on the problem partition function Z , a quantity often difficult to calculate^{19–21}, demanding computationally time consuming methods²². Obviously, approximations for the g 's can be used (e.g., as in Ref.¹⁵). But so the ST efficiency can be dramatically hindered, once the weights themselves can create certain bias for the sampling. For instance, they may lead to unbalanced sorted temperatures, given rise to a non-ergodic visit of the phase-space if the probabilities to pick the lower T_n 's are too high. On the other hand, if the more frequent T 's are the greater ones, the generated set of microstates cannot properly characterize the

system features at $T = T_1$, the actual temperature of interest. Such technical aspects associated to the g 's are even more delicate for first order phase transitions, a situation rarely analyzed with the ST^{6,23}.

Given the previous comments, our purpose in this contribution is twofold. First, to present a numerically simple – yet quite accurate – procedure to obtain the weight factors g , thus making the ST algorithm easier to implement, e.g., by avoiding involving recursive protocols²¹. This is accomplished with a method proposed in Ref.¹⁹, where Z is calculated directly from the transfer matrix largest eigenvalue ($\lambda^{(0)}$), straightforward to compute from Monte Carlo simulations. The key point is that although $\lambda^{(0)}$ gives the exact Z only at the thermodynamical limit, i.e., for infinite systems, the convergence is very fast. So, even for a relatively small system (as will be illustrated in the examples), any difference between its exact Z and that from $\lambda^{(0)}$ can be neglected and for all practical reasons the approach leads to the correct g 's. Second, to consider the ST for the already mentioned difficult case of first-order transitions, showing that the ST is also a helpful tool to address such regime, a possibility barely explored in the literature.

The work is organized as the following. We review the ST algorithm and how to calculate g from the transfer matrix in Section II. Also in Section II we exemplify the procedure efficiency by computing the partition function for the Ising model, a system for which Z can be obtained exactly. In Section III and IV we compare the present with other well established methods to study first-order phase transitions, taking as case studies the Blume-Capel, Blume-Emery-Griffiths (BEG) and Bell-Lavis models. Finally, remarks and the conclusion are drawn in Section V.

II. THE ST AND THE CALCULATION OF g

As mentioned in the Introduction, the ST algorithm is generally implemented as two steps procedure, repeated a given number of times. First, at a temperature $T_{n'}$ ($n' = 1, 2, \dots, N$), a standard Metropolis prescription is used to promote the transition $\sigma' \rightarrow \sigma''$ with the probability $P_{\sigma' \rightarrow \sigma''} = \min\{1, \exp[-\beta_{n'}(\mathcal{H}(\sigma'') - \mathcal{H}(\sigma'))]\}$ (for σ representing the system microscopic configurations). Second, an attempt to change the replica temperature (from $T_{n'}$ to $T_{n''}$) is made according to

$$p_{n' \rightarrow n''} = \min\{1, \exp[(\beta_{n'} - \beta_{n''})\mathcal{H}(\sigma) + (g_{n''} - g_{n'})]\}. \quad (1)$$

In Eq. (1), \mathcal{H} is the problem Hamiltonian, σ the actual microscopic state, and $n'' = 1, \dots, N$ arbitrary, so non-adjacent temperatures changes are allowed. Moreover, $\beta = 1/(k_B T)$ with k_B always set equal to 1 hereafter.

We observe that $p_{n' \rightarrow n''}$ is strongly dependent on the weights g 's. Indeed, for an appropriate sampling the evolution should uniformly visit all the established temperatures, which is the case when $g_n = \beta_n f_n$ for f_n the free-energy per volume V at T_n . Recalling the relation $\beta_n f_n = -\ln[Z_n]/V$, we see that the calculation of g is not a trivial task: neither the partition function nor the free-energy can be obtained directly from MC simulations since there are no thermodynamic quantities whose averages lead to Z and f . For this reason some alternative methods have been proposed^{15,24,25}. Here we shall consider a rather simple numerical approach to compute f_n ¹⁹, based on the transfer matrix \mathcal{T} largest eigenvalue $\lambda^{(0)}$.

Briefly, at the thermodynamic limit it holds true that (see details in the Appendix)

$$Z_n = (\lambda_n^{(0)})^K, \quad (2)$$

with $K \sim V^{1/d}$ and d the spatial dimension. To obtain $\lambda^{(0)}$ is straightforward. In fact, suppose for definiteness a 2D system with K layers of L sites each, so $V = L \times K$. Next, consider the full Hamiltonian decomposed as

$$\mathcal{H} = \sum_{k=1}^{k=K} \mathcal{H}(S_k, S_{k+1}), \quad (3)$$

where $S_k \equiv (\sigma_{1,k}, \sigma_{2,k}, \dots, \sigma_{L,k})$ represents the state configuration of the k -th layer. We further assume periodic boundary conditions, or $S_{K+1} = S_1$. The transfer matrix is defined (Appendix) so that its elements read¹⁹

$$\mathcal{T}(S_k, S_{k+1}) = \exp[-\beta \mathcal{H}(S_k, S_{k+1})]. \quad (4)$$

Then, as shown in the Appendix, we have $(\mathcal{T}(S_k, S_{k+1} = S_k) \equiv \mathcal{T}(S_k))$

$$\lambda^{(0)} = \langle \mathcal{T}(S_k) \rangle / \langle \delta_{S_k, S_{k+1}} \rangle. \quad (5)$$

This expression enables one to calculate the largest eigenvalue $\lambda^{(0)}$ of \mathcal{T} in terms of the averages $\langle \mathcal{T}(S_k) \rangle$ and $\langle \delta_{S_k, S_{k+1}} \rangle$, with $\delta_{S_k, S_{k+1}} = 1$ ($\delta_{S_k, S_{k+1}} = 0$) if the layers S_k and S_{k+1} are equal (different). We also should mention that $\langle \mathcal{T}(S_k) \rangle$ and $\langle \delta_{S_k, S_{k+1}} \rangle$ can be evaluated from quite standard MC simulations.

As the final step, the weights follow from

$$g = -\ln[\lambda_n^{(0)}]/L. \quad (6)$$

A relevant issue is that even though Eq. (2) is exactly only for infinite size systems, if L (or K) is not too small the relation is extremely accurate. Hence, for any practical purpose Eq. (6) gives the correct g , as we are going to illustrate in the next Sections.

In this way, we can summarize the proposed approach as the following. First, with Eqs. (5)-(6) one evaluates the partition function and consequently the free-energy weights (at the temperatures $\{T_n\}$) from usual MC simulations. Second, having the correct g 's, one just implements the ST algorithm as previously explained.

Finally, we comment on three important technical issues. The first is related to the query: how can standard MC simulations lead to good values for g around first-order phase transition if then Metropolis algorithm usually yields unbalanced samplings? The answer relies on the fact that the free-energies are all equal at such regime of phases coexistence. Hence, even a biased microscopic sampling will result in accurate free-energies and consequently appropriate g 's. On the other hand, the metastability typical of T 's in the vicinity of the transition temperature can difficult the determination (with the necessary precision) of the function $Z \times T$ in such interval. Thus, derivatives of Z with respect to distinct parameters, representing different thermodynamic quantities, will give poor results. So, a second point is that the transfer matrix alone is not a reliable method to study first-order phase transitions. Lastly, we mention that in the limit of large systems and high temperatures $\langle \delta_{S_k, S_{k+1}} \rangle$ is small, since the probability for the configurations S_k and S_{k+1} to be the same is very low. As a consequence, one may get bad estimations for the weights. In this case, a possible way to circumvent the problem is to decrease the size L of each layer and to increase the number of layers, maintaining the volume $V = L \times K$ constant (see also the discussion in the Section V).

A. An example: the partition function for the Ising model

Just to verify how good is the Eq. (2) for finite size systems, we consider the Ising model, whose partition function can be calculated exactly. The Hamiltonian is

$$\mathcal{H} = -J \sum_{\langle i,j \rangle} \sigma_i \sigma_j - H \sum_i \sigma_i, \quad (7)$$

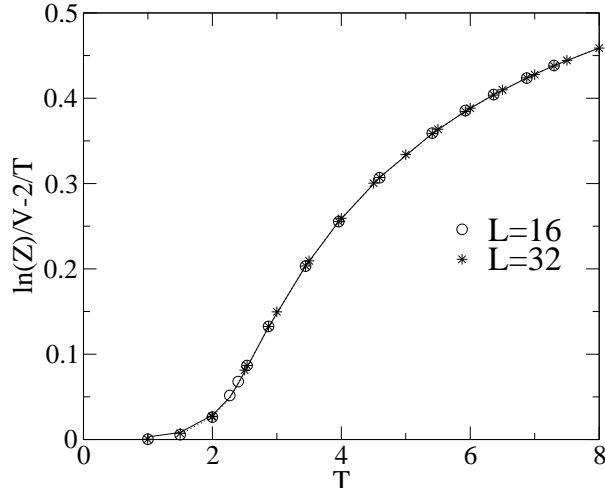


FIG. 1. For the Ising model, the partition function versus T calculated exactly²⁶ and from Eq. (2) (symbols), with the parameters as in the text. The exact solutions, the lines, for $L = 16$ (continuous) and $L = 32$ (dotted) are almost indistinguishable.

where $\langle i, j \rangle$ denotes nearest-neighbors pairs i and j in a lattice of $V = L^d$ sites. At each site i , the spin variable assumes the values $\sigma_i = \pm 1$. J is the interaction energy and H is the magnetic field. For a square lattice ($d = 2$), $\mathcal{T}(S_k)$ yields

$$\mathcal{T}(S_k) = \exp \left[\beta \left(\sum_{l=1}^L J (1 + \sigma_{l,k} \sigma_{l+1,k}) + H \sigma_{l,k} \right) \right]. \quad (8)$$

Numerical calculations have been performed for $H = 0$ (and in units of J). For $L = 16$ and $L = 32$, Fig. 1 compares the exact partition function for a finite system (obtained from the solution in Ref.²⁶) with that calculated from Eq. (2). The agreement is indeed remarkable, indicating that even for relatively small systems, Z and therefore f are already very close to their values at the thermodynamic limit.

Since the above system presents a very well known and simple first-order phase transition (for $H = 0$ and $T < T_c$), we prefer to address such regime, our focus in this contribution, for other models in the following Sections.

III. THE LATTICE-GAS MODEL WITH VACANCIES (BEG)

The lattice-gas with vacancies (BEG) model is given by the Hamiltonian ($\sigma = 0, \pm 1$)

$$\mathcal{H} = - \sum_{\langle i, j \rangle} (J \sigma_i \sigma_j + K \sigma_i^2 \sigma_j^2) - \sum_i (H \sigma_i - D \sigma_i^2), \quad (9)$$

for which the transfer matrix $\mathcal{T}(S_k)$ elements are

$$\mathcal{T}(S_k) = \exp \left[\beta \sum_{l=1}^L \left((H + J \sigma_{l+1,k}) \sigma_{l,k} + (J - D + K (1 + \sigma_{l+1,k}^2)) \sigma_{l,k}^2 \right) \right]. \quad (10)$$

For the values of K/J we are going to consider here and at low temperatures, if D is small, the system presents an ordered phase. When D increases, a gas phase takes place. These regimes are separated by a strong first-order phase transition at $D = D^*$. For simplicity, hereafter all the quantities will be given in units of J .

A. The Blume-Capel model

For the Blume-Capel case, $K = 0$, accurate estimates for f (which directly gives the ST weights once $g = \beta f$) is available from the very efficient Wang-Landau method. We then compare in Fig. 2 the free-energy from our proposed procedure with that from Wang-Landau's²⁷, considering $K = 0$, $L = 32$ and different D 's. As for the Ising model, again we see an excellent agreement (even for $D = 1.965$, the value corresponding to the tricritical point for T about 0.609). We also have explicit tested smaller L 's (down to 12), always obtaining very good results. So, the exact g 's for the ST are adequately (and easily) obtained from the transfer matrix approach.

To study the Blume-Capel model around first-order phase transition, we perform finite size scaling analysis using the PT algorithm. We first recall that according to a rigorous theory of first-order phase transitions at low temperatures²⁸, all thermodynamic quantities should scale with V . Then, for $Q = \sum_{i=1}^V \sigma_i^2$, in Fig. 3 we show the order parameter $q = \langle Q \rangle / V$ and the isothermal susceptibility $\chi_T = (k_B T)^{-1} (\langle Q^2 \rangle - \langle Q \rangle^2) / V$ as functions of D for three system sizes L . The transition point can be estimated, for instance, from the peak position in the susceptibility or in the specific heat curves. Here we obtain D^* through the location of the distinct L isotherms crossing^{9,29-31}. We find that for $T = 0.50$ all the isotherms cross at $D^* = 1.9879(1)$, which closely agree with the values $T = 0.499(3)$ and $D^* = 1.992(1)$ in Ref.²⁷. In addition, the good collapse of the data in the insets, plotted as $q \times (D - D^*) V$ and as $\chi_T / V \times (D - D^*) V$, illustrates the adequacy of the ST to locate transition points. Of course, other exact implementations of the ST, like that in Ref.²¹, would also solve the problem, however, by means of more complicated protocols, thus demanding longer computational times.

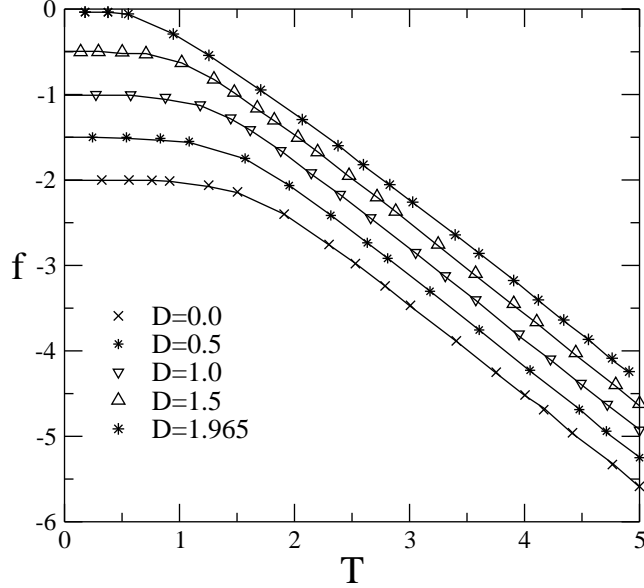


FIG. 2. For the Blume-Capel model, the free-energy versus T for different D obtained from the present approach (symbols) and from the Wang-Landau method (continuous lines).

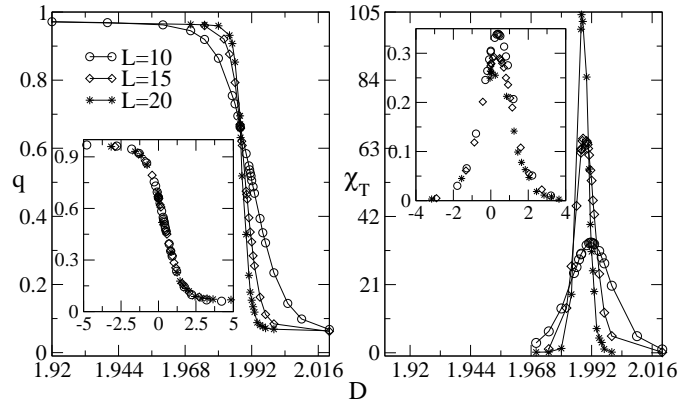


FIG. 3. For the Blume-Capel model, the order parameter q and the isothermal susceptibility χ_T versus D for different system sizes at $T = 0.5$. The insets show the collapsed data, respectively, plotted as $q \times (D - D^*) V$ and $\chi_T / V \times (D - D^*) V$.

B. The full, $K \neq 0$, BEG model

Next, we briefly comment on the full BEG model, i.e., $K \neq 0$. Generally, approaches based on cluster algorithms are known to be very appropriate for lattice-gas systems⁷. Nevertheless, it is also a fact that first-order phase transitions for some special K 's, like $K = 3.3$, can be a little trick to solve. So, modifications in the cluster method are necessary⁸.

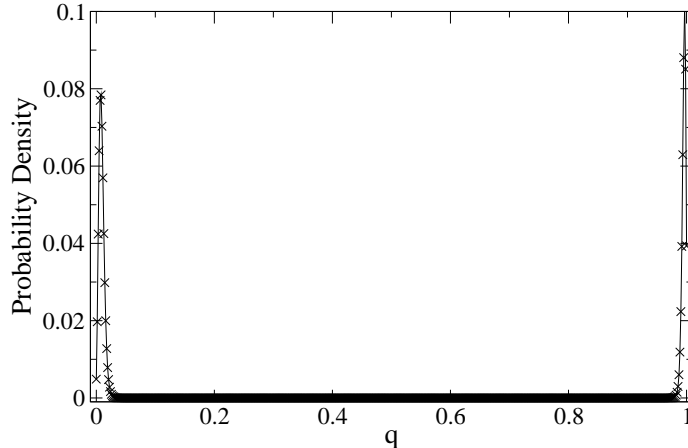


FIG. 4. For the BEG model, with $K/J = 3.3$ and parameters as in the text, the probability distribution histogram of the order parameter q . The continuous line is a guide for the eyes.

In the absence of calculations of f and Z when $K = 3.3$ in the literature (for a explicit comparison), in Fig. 4 we just present the probability distribution histogram for the order parameter q , considering $D = 8.605$, $T = 1.50$ and a small lattice of $L = 25$. From the two peaks with very similar heights, we see that the simulations are able to cross the large free-energy barriers at the phase coexistence. On the other hand, from an usual Metropolis simulations, the system would be trapped in metastable states, evolving to the stable phases only after very large MC steps. We should mention that qualitatively our results agree quite well with those in Fig. 1 (b) of Ref.⁸ for very similar parameters (actually, there the authors use a bigger lattice of $L = 32$ at $T = 1.50$, with $D = 8.6035$). We do not make a direct quantitative comparison, e.g., by digitalizing the results in Ref.⁸, simple because in the mentioned figure the scales are not explicitly given. By setting $L = 32$ (for which the eigenvalue method is even better because the greater L), we also have found a balanced bimodal distribution at the coexistence, with $D \approx 8.6035$ as in Ref.⁸.

As a final observation, we recall that $K = 3.0$ has been extensively studied under different approaches^{9,29,30}. In particular, it has been shown³² that for this parameter value, the ST is an efficient method to study the first-order phase transition for 2D square lattices as small as $L = 20$.

IV. THE BELL-LAVIS MODEL

As a last example, we consider the Bell-Lavis water model^{33,34}. It is defined on a triangular lattice, whose occupational variable σ_i ($i = 1, 2, \dots, V$) takes the values 1 (0) if the site is (is not) occupied by a water molecule. Moreover, each molecule is described by an orientational state, indicating to which nearest neighbor a hydrogen bonding can be formed. So, for a non-empty site i , we define the quantity τ_i^{ij} , where j runs over the first neighbors j of i . If there is a bonding arm pointed from i towards j , then $\tau_i^{ij} = 1$, otherwise $\tau_i^{ij} = 0$. Two adjacent molecules always interact via Van der Waals forces, whereas they do form hydrogen bonds provided $\tau_i^{ij} \times \tau_j^{ji} = 1$.

The model is described, in the grand-canonical ensemble, by the Hamiltonian

$$\mathcal{H} = - \sum_{\langle i,j \rangle} \sigma_i \sigma_j (\epsilon_{hb} \tau_i^{ij} \tau_j^{ji} + \epsilon_{vdw}) - \mu \sum_i \sigma_i, \quad (11)$$

where μ is the chemical potential and ϵ_{vdw} and ϵ_{hb} are, respectively, the Van der Waals and hydrogen bonds interaction energies. The Van der Waals force tends to increase the system density by filling the lattice with molecules. On the other hand, the hydrogen bond interaction essentially favors an increasing in the hydrogen bonds, so it effectively may limit the molecule density if μ is negative and small. Finally, the $\mathcal{T}(S_k)$ elements are given by

$$T(S_k) = \exp \left[\sum_{i=1}^L \left(\sigma_{i,k} (\sigma_{i,k} + 2\sigma_{i+1,k}) (\epsilon_{vdw} + \epsilon_{hb} \tau_{i,k} \tau_{i+1,k} + \mu) \right) \right]. \quad (12)$$

The Hamiltonian in Eq. (11) exhibits a very rich phase diagram. For instance, recent numerical simulations³⁵ show that the parameter conditions allowing the existence of two stable liquid phases take place when the hydrogen bonds are at least three times higher than the Van der Wall interaction, or $\zeta \equiv \epsilon_{vdw}/\epsilon_{hb} < 1/3$. In such case, for low negative μ values the system presents only a gas phase. By increasing μ a low-density-liquid-phase (LDLP) arises. In the limit of higher chemical potentials, we have a high-density-liquid-phase (HDLP). At $T = 0$, the LDLP (HDLP) has a global density of $\rho = 2/3$ ($\rho = 1$), with the hydrogen bond density per molecule being $\rho_{hb} = 3/2$ ($\rho_{hb} = 1$). Furthermore³⁵, both phase transitions are of first-order: that between the gas and the *LDLP* occurring at $\mu^* = -3(1 + \zeta)/2$ and that between the LDLP and HDLP at $\mu^* = -6\zeta$. For $T > 0$, the former remains first-order, ending at a tricritical point, whereas the latter becomes second-order, belonging to the Ising universality class³⁵.

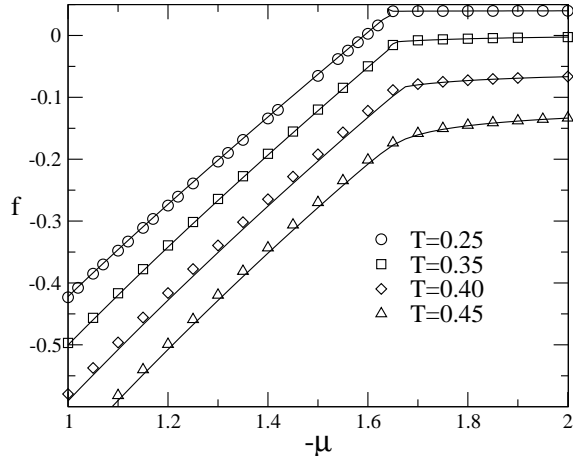


FIG. 5. For the Bell-Lavis model with $L = 18$, $f \times \mu$ obtained from the integration of the Gibbs-Duhem relation (continuous lines) and from the largest eigenvalue of \mathcal{T} (symbols). The different curves have been offset for a better visualization.

Next, we will focus on the first-order phase transition case, gas-LDLP, assuming $\zeta = 1/10$ and presenting all the results in units of ϵ_{hb} . First, we test the efficiency of the transfer matrix to yield the free-energies, hence the weights for the ST. In Fig. 5 we compare some values of f calculated from the \mathcal{T} approach with those obtained from numerical integration of the Gibbs-Duhem equation, $S dT - V dp + N d\mu = 0$, at fixed temperatures. Thus, $dp = \rho d\mu$ where the pressure is related to the free-energy per volume (grand-canonical) by the expression $f = -p$. As it can be seen, even for a small lattice size of $L = 18$ and low T 's, the agreement is very good.

Now, we assume a lattice of $L = 24$ and a rather small $T = 0.25$, difficult to simulate by standard one-flip algorithms. In Fig. 6 we plot the density ρ (the order parameter) as function of the chemical potential μ (the control parameter) around the phase transition point. We consider both the ST as well as an usual Metropolis algorithm. Contrary to the latter, the ST predicts the phase transition without displaying any hysteresis. In fact, hysteresis is a characteristic behavior of methods not able to properly sample the system when the phase space presents high free-energy barriers. Also, for the low T considered, the transition μ^* should not be too different from -1.65 , the thermodynamic value at $T = 0$ when $\zeta = 1/10$. Indeed, an expectation confirmed by Fig. 6.

Due to the lack of studies discussing first-order phase transition for the Bell-Lavis model (either by means of general or dedicated methods), here we compare the proposed ST algo-

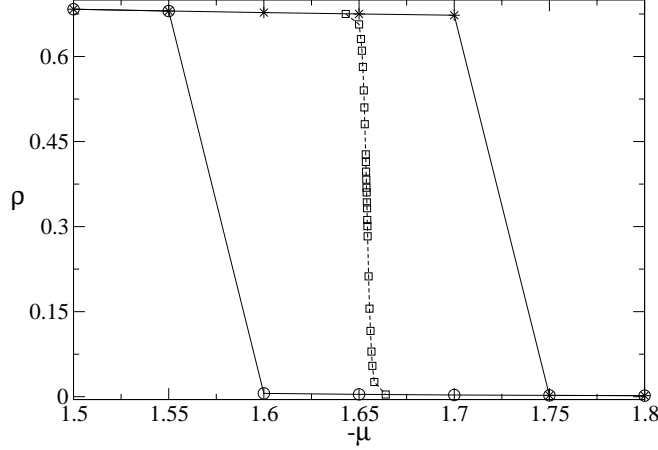


FIG. 6. For the Bell-Lavis model with $L = 24$ and at $T = 0.25$, q versus μ calculated from the ST (square) and from a common Metropolis method. The hysteresis is due to the latter algorithm difficulty in properly sampling the system.

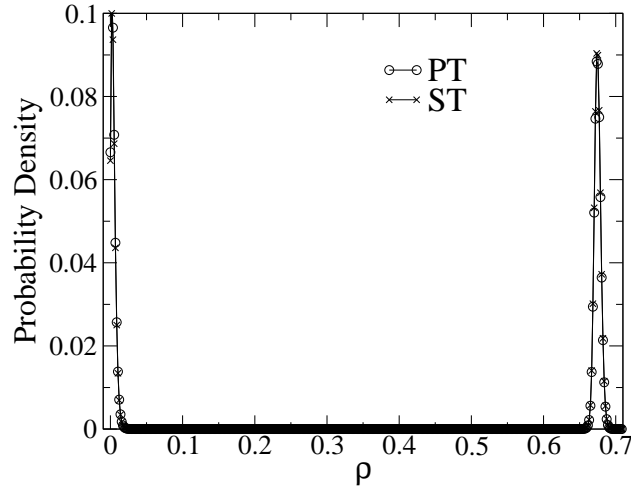


FIG. 7. For the Bell-Lavis model with $T = 0.25$, $L = 24$ and $\mu = -1.6533$, the probability distribution histogram of the order parameter ρ calculated from the ST and PT methods. The continuous line is a guide for the eyes.

rithm with calculations based on the parallel tempering (PT) approach, recently shown to be a very efficient tool to analyze such thermodynamical regime^{29,32,36,37}. In Fig. 7 we plot the histogram of the order parameter ρ at the phase coexistence for $T = 0.25$ and $L = 24$. In ‘tuning’ the chemical potential so to have the two peaks of about the same high, we find $\mu = -1.6533$. We emphasize the quite good agreement between the methods, both being able to circumvent metastable states and to promote frequent visits between the gas phase

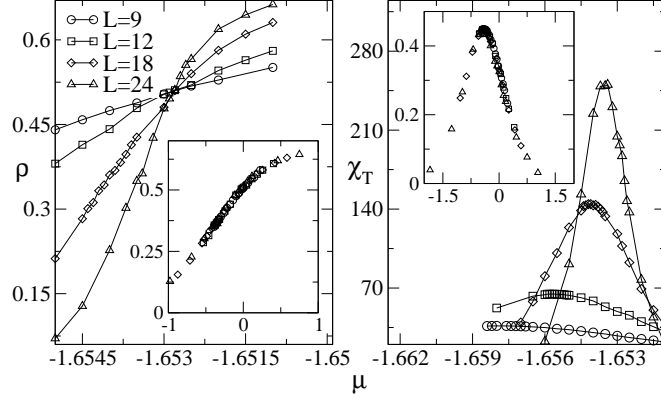


FIG. 8. For the Bell-Lavis model, the order parameter ρ and compressibility χ_T versus μ for different system sizes at $T = 0.25$. The insets show the collapsed data, respectively, plotted as $\rho \times (\mu - \mu^*) V$ and $\chi_T/V \times (\mu - \mu^*) V$.

and the LDLP.

We finally perform a finite-size analysis to determine the phase coexistence. We plot in Fig. 8 the order parameter ρ and the compressibility χ_T as functions of μ , assuming different system sizes L and fixed $T = 0.25$. Note that we obtain very smooth curves and that χ_T exhibits sharper peaks as L increases. Moreover, all the isotherms for the density ρ cross each other at the same point $\mu^* = -1.6528(1)$ (as it should be²⁸, a value close but smaller than that for a finite system, e.g., the one in Fig. 7). After locating μ^* with accuracy, we can perform a rescaling of the data, finding a very good collapse by plotting $\rho \times (\mu - \mu^*) V$ and $\chi_T/V \times (\mu - \mu^*) V$. Such results confirm the amenability of the present procedure for estimating the transition points in discontinuous phase transitions.

V. REMARKS AND CONCLUSION

In this paper we have considered an alternative simple protocol to calculate very accurate free-energy weights for the ST (simulated tempering) method. It consists in estimating f by means of the largest eigenvalue of the transfer matrix¹⁹, a quantity directly obtained from standard Monte Carlo simulations. To illustrate the approach, we have addressed strong first-order phase transitions for different lattice models, namely, Blume-Capel, BEG and Bell-Lavis. In such regime, distinct regions of the phase space can be separated by high entropic barriers, thus demanding efficient sampling procedures. In all cases, our results have

agreed quite well with available precise calculations in the literature, with the advantage that our ST has a simple implementation. Next, two remarks are in order.

First, as already mentioned, an advantage of the present implementation is the relative low computation cost in obtaining the refined weights – based on standard MC simulations. It is not our purpose here a detailed benchmark comparison between different methods. Nevertheless, without going into the merit of the (good) performance of other approaches such as Wang-Landau and parallel tempering (for the later, see, e.g., Ref.³²), we observe the following. Algorithmically speaking, in principle the ST may be faster since it does not demand: either (i) to know the density of states as in the Wang-Landau (usually a hard task, e.g., in our examples involving 3^V configurations); or (ii) to simultaneously simulate many replicas as in the PT (in the ST only one system realization is considered).

Second, by increasing too much the system size, the accepting probabilities for the temperature exchanges decrease, eventually leading to a poor estimation for the thermodynamic quantities (but for a possible way to assuage it, see the end of Section II). In fact, the difficulty in simulating large systems is not a peculiarity of the ST. It also may be the case in others methods like the PT and Wang-Landau. A finite-size analysis circumvent this problem, but in practice should use L 's up to a certain maximum value L_m , for which the considered method still works well. The crucial point is whether L_m allows a correct extrapolation to the thermodynamic limit. In our many examples, for L around 25 we already can predict this limit. But other situations would require, say, $L = 100$, which in principle could be calculated with our approach if we use a larger set of temperatures $\{T_n\}$, but with $\Delta T = (T_n - T_1)$ fixed. Presently, such issue is under investigation and will be the subject of a forthcoming publication.

In summary, the examples given show that the ST algorithm allied to our straightforward way to calculate the weights is able to deal with free-energy barriers, common at the phase coexistence, and therefore can be very useful in characterizing first-order phase transitions.

ACKNOWLEDGEMENTS

We acknowledge researcher grants from CNPq. Financial support is also provided by CNPq-Edital Universal, Fundação Araucária and Finep/CT-Infra.

Appendix A: The transfer matrix method to calculate Z

Here we present a general overview on the transfer matrix method¹⁹, and how it can be used to calculate Z .

Consider a general Hamiltonian of a regular lattice, written as

$$\mathcal{H} = \sum_{k=1}^K \mathcal{H}(S_k, S_{k+1}), \quad (\text{A1})$$

for $S_k \equiv (\sigma_{1,k}, \sigma_{2,k}, \dots, \sigma_{L,k})$ the state configuration of the k -th layer (each having L sites). Also, assume periodic boundary conditions, so that $S_{K+1} = S_1$.

From the definition of the (grand-canonical) partition function Z , we have that the probability $P(S_1, S_2, \dots, S_K)$ for the layer 1 to have the configuration S_1 , the layer 2 the configuration S_2 , and so on, is given by ($\beta = 1/(k_B T)$)

$$P(S_1, \dots, S_K) = \frac{\exp[-\beta \mathcal{H}(S_1, S_2)] \times \dots \times \exp[-\beta \mathcal{H}(S_{K-1}, S_K)] \times \exp[-\beta \mathcal{H}(S_K, S_1)]}{Z}. \quad (\text{A2})$$

We then can define the transfer matrix \mathcal{T} such that its elements $\mathcal{T}(S', S'')$ are equal to $\exp[-\beta \mathcal{H}(S', S'')]$, for S' and S'' being the configurations of two successive neighbor layers. Hence, the r.h.s. of Eq. (A2) reads $\mathcal{T}(S_1, S_2) \dots \mathcal{T}(S_K, S_1)/Z$.

Next, since

$$\sum_{S_1, \dots, S_K} P(S_1, \dots, S_K) = 1, \quad (\text{A3})$$

it naturally follows that

$$Z = \sum_{S_1, \dots, S_K} \mathcal{T}(S_1, S_2) \mathcal{T}(S_2, S_3) \dots \mathcal{T}(S_{K-1}, S_K) \mathcal{T}(S_K, S_1). \quad (\text{A4})$$

But observe that $\sum_{S_k} \mathcal{T}(S_{k-1}, S_k) \mathcal{T}(S_k, S_{k+1}) = \mathcal{T}^2(S_{k-1}, S_{k+1})$, with this last term denoting the element (S_{k-1}, S_{k+1}) of the matrix \mathcal{T}^2 . Thus, using such relation recursively in Eq. (A4), one finds

$$Z = \sum_{S_1} \mathcal{T}^K(S_1, S_1) = \text{Tr}[\mathcal{T}^K]. \quad (\text{A5})$$

If now we calculate all the eigenvalues $\{\lambda^{(m)}\}$ of \mathcal{T} , from basic linear algebra we get

$$Z = \sum_m (\lambda^{(m)})^K. \quad (\text{A6})$$

Finally, for K large enough, the most important contribution in Eq. (A6) comes from the largest eigenvalue of \mathcal{T} , $\lambda^{(0)}$, and thus we recover Eq. (2) of Sec. II (which is exact in the thermodynamic limit of $K \rightarrow \infty$).

To derive an expression for $\lambda^{(0)}$, observe that the marginal probabilities

$$P(S_1) = \sum_{S_2, \dots, S_N} P(S_1, S_2, S_3, \dots, S_N), \quad P(S_1, S_2) = \sum_{S_3, \dots, S_N} P(S_1, S_2, S_3, \dots, S_N), \quad (\text{A7})$$

are readily obtained from Eq. (A2) and from proper products of the \mathcal{T} matrix elements, or ($S_1 = S'$, $S_2 = S''$)

$$P(S') = \frac{\mathcal{T}^K(S', S')}{Z}, \quad P(S', S'') = \frac{\mathcal{T}(S', S'') \mathcal{T}^{K-1}(S'', S')}{Z}. \quad (\text{A8})$$

For $|m\rangle$ being the eigenvector associated to the eigenvalue $\lambda^{(m)}$ of \mathcal{T} , we have that the usual spectral expansion of an operator, $\mathcal{T} = \sum_m \lambda^{(m)} |m\rangle\langle m|$, yields

$$\mathcal{T}(S', S'') = \sum_m \lambda^{(m)} \phi^{(m)}(S') \phi^{(m)*}(S''), \quad (\text{A9})$$

for $\phi^{(m)}(S')$ an element of $|m\rangle$ in the representation of the layer configurations $\{S\}$. Therefore

$$P(S') = \frac{1}{Z} \sum_m (\lambda^{(m)})^K \phi^{(m)}(S') \phi^{(m)*}(S'), \quad (\text{A10})$$

and

$$P(S', S'') = \frac{1}{Z} \mathcal{T}(S', S'') \sum_m (\lambda^{(m)})^{K-1} \phi^{(m)}(S') \phi^{(m)*}(S''). \quad (\text{A11})$$

Again, considering K large enough, Eqs. (A10) and (A11) can be approximated by

$$P(S') = \phi^{(0)}(S') \phi^{(0)*}(S'), \quad P(S', S'') = \frac{1}{\lambda^{(0)}} \mathcal{T}(S', S'') \phi^{(0)}(S') \phi^{(0)*}(S''). \quad (\text{A12})$$

Setting $S' = S''$ in Eq. (A12), we arrive at

$$P(S', S') = \sum_{S''} \delta_{s', s''} P(S', S'') = \frac{1}{\lambda^{(0)}} \mathcal{T}(S', S') P(S'). \quad (\text{A13})$$

Lastly, summing Eq. (A13) over S' and identifying the averages (for $\mathcal{T}(S') \equiv \mathcal{T}(S', S')$)

$$\langle \delta_{S', S''} \rangle = \sum_{S', S''} \delta_{s', s''} P(S', S''), \quad \langle \mathcal{T}(S') \rangle = \sum_{S'} \mathcal{T}(S') P(S'), \quad (\text{A14})$$

we obtain Eq. (5).

REFERENCES

- ¹J. C. Mauro, P. K. Gupta, and R. J. Loucks, *J. Chem. Phys.* **126**, 184511 (2007).
- ²H. G. Katzraber, S. Trebst, D. A. Huse and M. Troyer, *J. Stat. Mech.* **3**, P031018 (2006).
- ³S. R. Williams and D. J. Evans, *J. Chem. Phys.* **127**, 184101 (2007).
- ⁴R. G. Palmer, *Adv. Phys.* **31**, 669 (1982).
- ⁵J. P. Neirotti, D. L. Freedman and J. D. Doll, *Phys. Rev. E* **62**, 7445 (2000).
- ⁶G. Besold, J. Risbo and O. G. Mouritsen, *Comput. Mat. Sci.* **15**, 311 (1999).
- ⁷W. Janke and S. Kappler, *Phys. Rev. Lett.* **74**, 212 (1995); M. B. Bouabci and C. E. I. Carneiro, *Phys. Rev. B* **54**, 359 (1996).
- ⁸A. Rachadi and A. Benyoussef, *Phys. Rev. B* **68**, 064113 (2003).
- ⁹C. E. Fiore and C. E. I. Carneiro, *Phys. Rev. E* **76**, 021118 (2007).
- ¹⁰G. Stolovitzky and B. J. Berne, *PNAS* **97**, 11164 (2000).
- ¹¹F. Wang and D. P. Landau, *Phys. Rev. Lett.* **86**, 2050 (2001); *ibid* *Phys. Rev. E* **64**, 056101 (2001).
- ¹²D. J. Earl and M. W. Deem, *Phys. Chem. Chem. Phys.* **7**, 3910 (2005).
- ¹³Y. Q. Gao, *J. Chem. Phys.* **128**, 134111 (2008)
- ¹⁴E. Marinari and G. Parisi, *Europhys. Lett.* **19**, 451 (1992).
- ¹⁵S. Park and V. S. Pande, *Phys. Rev. E* **76**, 016703 (2007).
- ¹⁶R. H. Swendsen and J.-S. Wang, *Phys. Rev. Lett.* **57**, 2607 (1986); K. Hukushima and K. Nemoto, *J. Phys. Soc. Jpn.* **65**, 1604 (1996); J.-S. Wang and R. H. Swendsen, *Prog. Theor. Phys. Suppl.* **157**, 317 (2005).
- ¹⁷B. A. Berg, *Comput. Phys. Commun.* **147**, 52 (2002).
- ¹⁸J. G. Kim, Y. Fukunishi, and H. Nakamura, *Chem. Phys. Lett.* **392**, 34 (2004); J. G. Kim, Y. Fukunishi, and H. Nakamura, *Phys. Rev. E* **69**, 021101 (2004); M. Fasnacht, R. H. Swendsen, and J. M. Rosenberg, *Phys. Rev. E* **69**, 056704 (2004).
- ¹⁹R. A. Sauerwein and M. J. de Oliveira, *Phys. Rev. B*, **52**, 3060 (1995).
- ²⁰D. P. Landau and K. Binder, *A Guide to Monte Carlo Simulations in Statistical Physics*, (Cambridge Univ. Press, Cambridge, 2000).
- ²¹C. Zhang and J. P. Ma, *J. Chem. Phys.* **129**, 134112 (2008).
- ²²Y. Okamoto, *J. Mol. Graph. Model.* **22**, 425 (2004).
- ²³U. H. E. Hansmann and Y. Okamoto, *J. Comput. Chem.* **18**, 920 (1997); M. Picco and

- F. Ritort, *Physica A* **250**, 46 (1998); G. Doge, K. Mecke, J. Moller, D. Stoyan and R. P. Waagepetersen, *Int. J. Mod. Phys. C* **15**, 129 (2004).
- ²⁴S. Park, *Phys. Rev. E* **77**, 016709 (2008).
- ²⁵X. Huang, G. R. Bowmann and V. S. Pande, *J. Chem. Phys.* **128**, 205106 (2008).
- ²⁶B. Kaufman, *Phys. Rev.* **76**, 1232 (1949); A. E. Ferdinand and M. E. Fisher, *Phys. Rev.* **185**, 832 (1969).
- ²⁷C. J. Silva, A. A. Caparica and J. A. Plascak, *Phys. Rev. E* **73**, 036702 (2006).
- ²⁸C. Borgs and R. Kotecky, *Phys. Rev. Lett.* **68**, 1734 (1992).
- ²⁹C. E. Fiore, *Phys. Rev. E* **78**, 041109 (2008).
- ³⁰C. E. Fiore, V. B. Henriques and M. J. de Oliveira, *J. Chem. Phys.* **125**, 164509 (2006).
- ³¹H. C. M. Fernandes, J. J. Arenzon and Y. Levin, *J. Chem. Phys.* **126**, 114508 (2007).
- ³²C. E. Fiore and M. G. E. da Luz, *Phys. Rev. E* **82**, 031104 (2010).
- ³³G. M. Bell and D. A. Lavis, *J. Phys. A* **3**, 568 (1970).
- ³⁴D. A. Lavis, *J. Phys. C* **6**, 1530 (1973).
- ³⁵C. E. Fiore, M. M. Szortyka, M. C. Barbosa and V. B. Henriques, *J. Chem. Phys* **131**, 164506 (2009).
- ³⁶P. Sengupta, A. W. Sandvik and D. L. Campbell, *Phys. Rev. B* **65**, 155113 (2002); E. Bittner and W. Janke *J. Phys. A* **41**, 395001 (2008). A. P. Young, S. Knysh and V. N. Smelyanskiy, *Phys. Rev. Lett.* **104**, 020502 (2010).
- ³⁷T. Neuhaus, M. P. Magiera and U. H. E. Hansmann, *Phys. Rev. E* **76**, 045701(R) (2007).